Spin Currents in a Coherent Exciton Gas

A. A. High,[1] A. T. Hammack,[1] J. R. Leonard,[1,*] Sen Yang,[1] L. V. Butov,[1] T. Ostatnický,[2] M. Vladimirova,[3] A. V. Kavokin,[3,4,5] T. C. H. Liew,[6] K. L. Campman,[7] and A. C. Gossard[7]

[1]*Department of Physics, University of California at San Diego, La Jolla, California 92093-0319, USA*
[2]*Faculty of Mathematics and Physics, Charles University in Prague, Ke Karlovu 3, 121 16 Prague, Czech Republic*
[3]*Laboratoire Charles Coulomb, Université Montpellier 2, CNRS, UMR 5221, F-34095 Montpellier, France*
[4]*School of Physics and Astronomy, University of Southampton, SO17 1BJ Southampton, United Kingdom*
[5]*Spin Optics Laboratory, State University of Saint Petersburg, 1 Ulianovskaya 198504, Russia*
[6]*Mediterranean Institute of Fundamental Physics, 31 via Appia Nuova, Rome 00040, Italy*
[7]*Materials Department, University of California at Santa Barbara, Santa Barbara, California 93106-5050, USA*
(Received 27 March 2013; published 11 June 2013)

We report the observation of spin currents in a coherent gas of indirect excitons. The realized long-range spin currents originate from the formation of a coherent gas of bosonic pairs—a new mechanism to suppress the spin relaxation. The spin currents result in the appearance of a variety of polarization patterns, including helical patterns, four-leaf patterns, spiral patterns, bell patterns, and periodic patterns. We demonstrate control of the spin currents by a magnetic field. We also present a theory of coherent exciton spin transport that describes the observed exciton polarization patterns and indicates the trajectories of the spin currents.

DOI: 10.1103/PhysRevLett.110.246403 PACS numbers: 71.35.−y, 72.25.Dc

Studies of electron spin currents in semiconductors led to the discoveries of the spin Hall effect [1–6], persistent spin helix [7], and spin drift, diffusion and drag [8–10]. An important role in spin current phenomena is played by spin-orbit (SO) coupling. It is the origin of the spin Hall effect and persistent spin helix. It also creates spin structures with the spin vector perpendicular to the momentum of the electrons in metals [11] and topological insulators [12–14]. While phenomena caused by SO coupling are ubiquitous in fermionic systems, they have yet to be explored in bosonic matter. Available experimental data for bosons include the optical spin Hall effect in photonic systems [15–17] and spin patterns in atomic condensates [18,19].

Here, we report the observation of spin currents in a system of matter bosons in semiconductors—indirect excitons. Excitons—bound pairs of electrons and holes—form a model system to study spin currents of bosons [20]. Spin-orbit coupling for an exciton originates from the combined Dresselhaus and Rashba effects for the electron and the hole [21–23]. An indirect exciton can be formed by an electron and a hole confined in separate quantum-well (QW) layers [see Fig. 1(a)]. The spatial separation reduces the overlap of electron and hole wave functions thus producing indirect excitons with lifetimes orders of magnitude longer than those of direct excitons [24,25]. Due to their long lifetimes, indirect excitons can travel over large distances before recombination [26] and can cool down below the temperature of quantum degeneracy and form a condensate [27].

The condensation of indirect excitons was predicted to cause the suppression of exciton scattering [24]. The measured strong enhancement of the exciton coherence length [27] experimentally shows the suppression of exciton scattering. The suppression of scattering results in the suppression of the Dyakonov-Perel and Elliott-Yafet mechanisms of spin relaxation [28]. Furthermore, the spatial separation between an electron and a hole suppresses the Bir-Aronov-Pikus mechanism of spin relaxation for indirect excitons [29,30]. The suppression of these mechanisms of spin relaxation results in a strong enhancement of the spin relaxation time in a condensate of indirect excitons. While the spin relaxation times of free fermions—electrons and holes—can be short [29], the formation of a coherent gas of their bosonic pairs results in a strong enhancement of their spin relaxation times. This mechanism to suppress the spin relaxation and facilitate long-range spin currents can be called coherent pairing.

Previous studies identified the external ring and localized bright spot (LBS) rings in the emission pattern of indirect excitons [see Fig. 1(c)] as sources of cold excitons [27]. These rings form on the boundaries between electron-rich and hole-rich regions; the former is created by current through the structure (specifically, by the current filament at the LBS center in the case of the LBS ring), whereas the latter is created by optical excitation [see Fig. 1(b)]; see Ref. [27] and references therein. In Ref. [27], we presented the studies of spontaneous coherence of indirect excitons in the ring region.

Here, we present the studies of spin currents and associated spin patterns around the sources of cold excitons—the rings. We present the observation of patterns of circular polarization, corresponding to spin perpendicular to the QW plane. We also show that the observed polarization

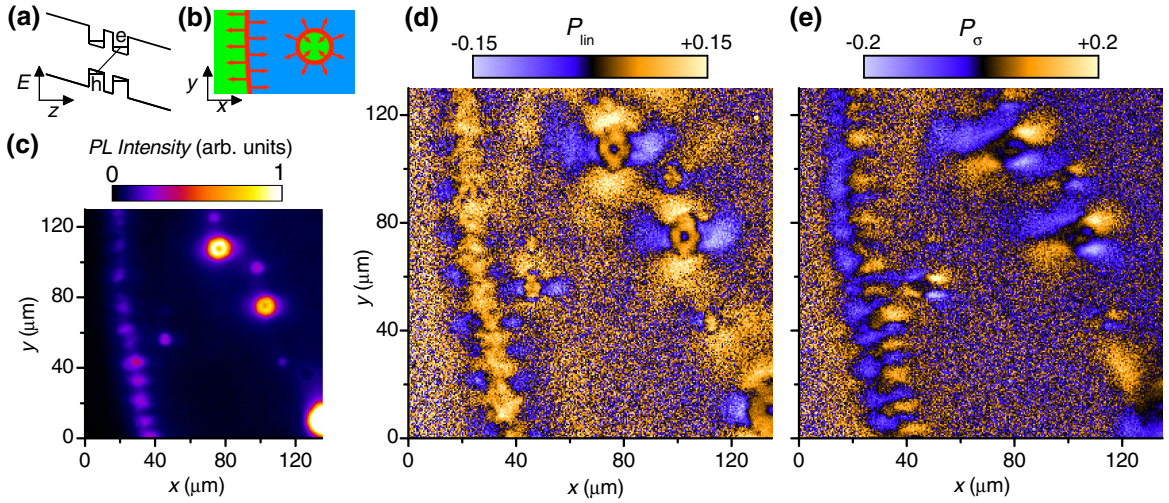

FIG. 1 (color online). Polarization patterns in exciton emission. (a) Diagram of the CQW: e, electron; h, hole. (b) Schematic of exciton formation in the external ring (left) and LBS ring (right); excitons (red) form on the boundary of hole-rich (blue) and electron-rich (green) areas. Exciton transport is indicated by red arrows. (c) A segment of the emission pattern of indirect excitons showing the external ring (left) and multiple LBS. (d),(e) Patterns of linear $P_{\rm lin} = (I_x - I_y)/(I_x + I_y)$ (d) and circular $P_\sigma = (I_{\sigma^+} - I_{\sigma^-})/(I_{\sigma^+} + I_{\sigma^-})$ (e) polarization of the emission of indirect excitons in the region shown in (c). $T_{\rm bath} = 0.1$ K.

patterns are controlled by a magnetic field: these data prove that the pattern of linear polarization corresponds to spin orientation rather than merely to the orientation of an exciton dipole. We also deduce trajectories of electron and hole spin currents from the measured polarization patterns.

The exciton polarization currents and associated spin textures are revealed by the polarization pattern of the emitted light measured by polarization-resolved imaging [see Figs. 1(d) and 1(e)]. Experiments are performed in an optical dilution refrigerator. The photoexcitation is nonresonant and spatially separated so that the exciton polarization is not induced by the pumping light.

The binding energy released at the exciton formation in the rings and the current filament at the LBS center heat the exciton gas. The former heating source depletes the exciton condensate in the rings [27]. The latter is so strong that no condensate forms in the LBS ring center and the exciton gas is classical there [27]. Excitons cool down with increasing distance r away from the heating sources so that they can approach the condensation temperature at $r = r_0$ where the condensation is detected by interferometric measurements [27].

The indirect excitons in a GaAs coupled quantum well structure (CQW) may have four spin projections on the z direction normal to the CQW plane: $J_z = -2, -1, +1, +2$. The states $J_z = -1$ and $+1$ contribute to left- and right-circularly polarized emission and their coherent superposition to linearly polarized emission, whereas the states $J_z = -2$ and $+2$ are dark [29]. The electron and hole spin projections on the z axis are given by J_z, while in-plane projections of electron and hole spins can be deduced from the off-diagonal elements of the exciton spin density matrix, which can be obtained from the measured polarization pattern (see the Supplemental Material [31]). The exciton states linearly polarized along the axes of symmetry are generally split due to in-plane anisotropy induced by the crystallographic axis orientation and strain.

The observed polarization patterns are qualitatively similar for both sources of cold excitons—the external ring and LBS ring. A LBS ring is close to a model radially symmetric source of excitons with a divergent (hedgehog) momentum distribution [see Fig. 1(b)] and we concentrate on the polarization textures around the LBS here. All LBS rings in the emission pattern show similar spin textures [see Figs. 1(d) and 1(e)].

A ring of linear polarization is observed around each LBS center [see Figs. 1(d) and 2(a)]. This ring is observed in the region $r < r_0$ where the exciton gas is classical. The linear polarization originates from the thermal distribution of excitons over the linearly polarized exciton states. Heating of the exciton gas by the current filament reduces the polarization degree in the LBS center and, as a result, leads to the appearance of a ring of linear polarization. No such polarization reduction is observed in the external ring, consistent with the absence of heating by current filaments in the external ring area [see Fig. 1(d)].

A helical exciton polarization texture that winds by 2π around the origin emerges in the LBS area at $r > r_0$ where the condensate forms (the latter is measured by shift interferometry); see Figs. 1(d), 2(a), and 2(c). The LBS exhibits a divergent hedgehog-shaped momentum distribution [see Fig. 3(d)]. The exciton polarization is perpendicular to exciton momentum [see Figs. 2(a) and 3(d)]. This produces vortices of linear polarization which emerge in concert with spontaneous coherence below the critical temperature

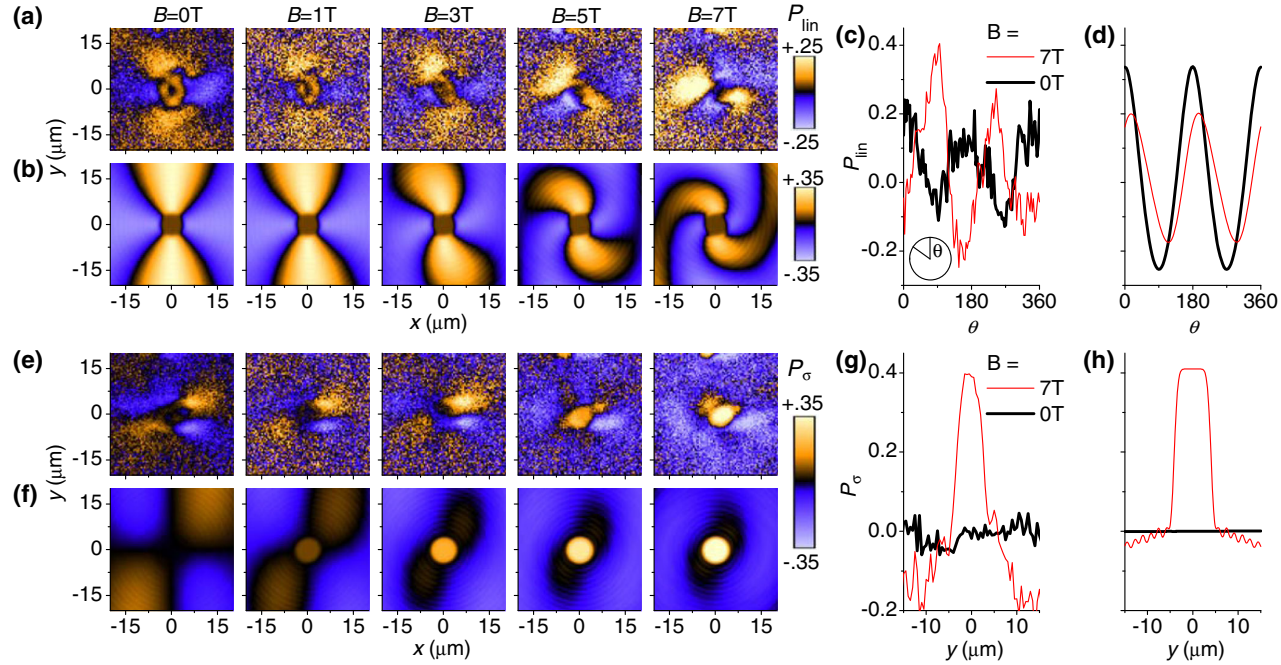

FIG. 2 (color online). Control of polarization patterns. Measured (a) and simulated (b) patterns of linear polarization of the emission of indirect excitons P_{lin} in the region of LBS for different magnetic fields perpendicular to the QW plane B. Measured (c) and simulated (d) azimuthal variation of P_{lin} at a distance from the LBS center $r = 9$ μm for $B = 0$ (black) and 7 T (red). Angles are measured from the y axis. Measured (e) and simulated (f) patterns of circular polarization of the emission of indirect excitons P_σ in the region of LBS for different B. Measured (g) and simulated (h) cross sections of P_σ at $x = 0$ for $B = 0$ (black) and 7 T (red). For all data, $T_{bath} = 0.1$ K; the LBS is at (105,75) in Fig. 1(c). See the Supplemental Material [31].

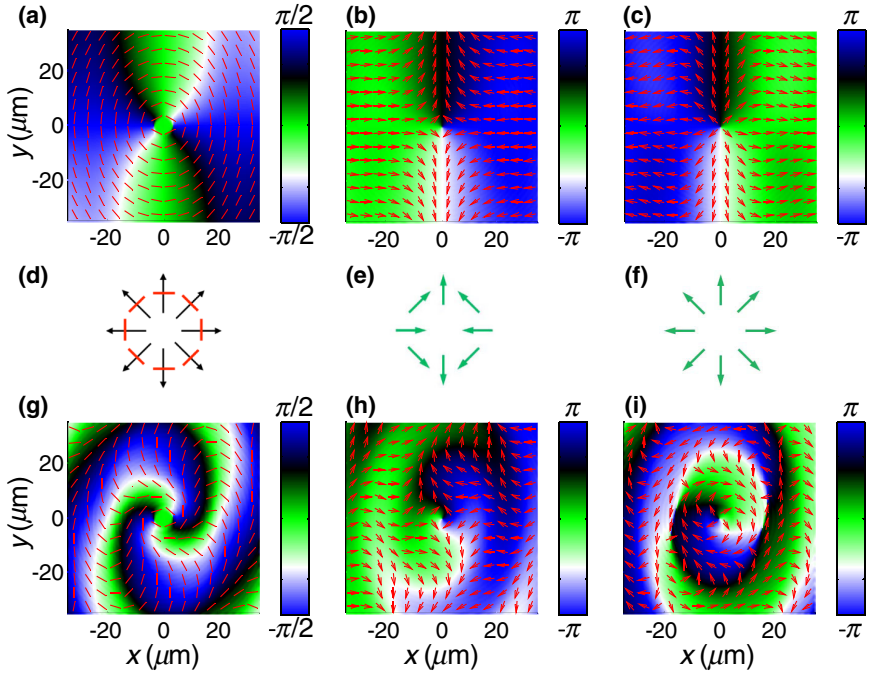

FIG. 3 (color online). Spin textures. Simulated in-plane exciton polarization (a), electron spin (b), and hole spin (c) patterns. (d) Schematic of exciton momentum (black arrows) and linear polarization (red lines) patterns. Schematic of effective magnetic fields given by the Dresselhaus SO interaction for electrons (e) and holes (f). Exciton polarization (g), electron spin (h), and hole spin (i) patterns in applied magnetic field $B = 7$ T. The lines (arrows) and the color visualize the orientation of the linear polarization (spin).

(see the Supplemental Material [31]). The observed radial exciton polarization currents are associated with spin currents carried by electrons and holes bound into excitons as detailed below.

Applied magnetic fields bend the spin current trajectories creating spiral patterns of linear polarization around the origin [see Figs. 2(a) and 2(c)]. The spiral direction of the exciton polarization current clearly deviates from the radial direction of the exciton density current [see Figs. 2(a) and 2(c)]. The control of the polarization patterns by a magnetic field shows that they are associated with spin.

Regular patterns are also observed in circular polarization [see Figs. 1(e) and 2(e)]. A LBS source of excitons generates a four-leaf pattern of circular polarization [see Figs. 1(e) and 2(e)]. This pattern vanishes with increasing temperature (see the Supplemental Material [31]). An applied magnetic field transforms the four-leaf pattern to a bell-like pattern of circular polarization with a strong circular polarization in the center and polarization inversion a few micrometers away from the center [see Figs. 2(e) and 2(g)].

Polarization patterns are also observed in the external ring region [see Figs. 1(d) and 1(e)]. At low temperatures, the macroscopically ordered exciton state (MOES) forms in the external ring. The MOES is characterized by a spatially ordered array of higher-density beads and is a condensate in momentum space [27]. The polarization texture in the external ring region appears as the superposition of the polarization textures produced by the MOES beads with each being similar to the texture produced by a LBS [see Figs. 1(d) and 1(e)]. A periodic array of beads in the MOES [see Fig. 1(c)] creates periodic polarization textures [see Figs. 1(d) and 1(e)]. The periodic polarization textures in the external ring region vanish above the critical temperature of the MOES (see the Supplemental Material [31]).

Below we present a theoretical model which describes the appearance of the exciton polarization textures and links them to spin currents carried by electrons and holes bound into bright and dark exciton states. This model is based on ballistic exciton transport out of the LBS origin and coherent precession of spins of electrons and holes. The former originates from the suppression of scattering and the latter from the suppression of spin relaxation in the condensate of indirect excitons. The states with different spins are split due to the splitting of linearly polarized exciton states and SO interaction, which is described by the Dresselhaus Hamiltonian $H_e = \beta_e(k_x^e\sigma_x - k_y^e\sigma_y)$ for electrons and $H_h = \beta_h(k_x^h\sigma_x + k_y^h\sigma_y)$ for holes [21–23] ($\mathbf{k}_{e,h}$ are electron and hole wave vectors given by $k_e = k_{\rm ex}m_e/(m_e + m_h)$ and $k_h = k_{\rm ex}m_h/(m_e + m_h)$, m_e and m_h are in-plane effective masses of the electron and heavy hole, respectively, $k_{\rm ex}$ is the exciton wave vector, $\beta_{e,h}$ are constants, and $\sigma_{x,y}$ are Pauli matrices). In the basis of four exciton states with spins $J_z = +1, -1, +2, -2$, the coherent spin dynamics in the system is governed by a model matrix Hamiltonian:

$$\hat{H} = \begin{bmatrix} E_b - (g_h - g_e)\mu_B B/2 & -\delta_b & k_e\beta_e e^{-i\phi} & k_h\beta_h e^{-i\phi} \\ -\delta_b & E_b + (g_h - g_e)\mu_B B/2 & k_h\beta_h e^{i\phi} & k_e\beta_e e^{i\phi} \\ k_e\beta_e e^{i\phi} & k_h\beta_h e^{-i\phi} & E_d - (g_h + g_e)\mu_B B/2 & -\delta_d \\ k_h\beta_h e^{i\phi} & k_e\beta_e e^{-i\phi} & -\delta_d & E_d + (g_h + g_e)\mu_B B/2 \end{bmatrix}, \quad (1)$$

where E_b and E_d are energies of bright and dark excitons in an ideal isotropic QW, and δ_b and δ_d describe the effect of in-plane anisotropy resulting in the splitting of exciton states linearly polarized along the axes of symmetry. The angle φ is measured from the x axis. The details of this model are presented in the Supplemental Material [31]. Exciton propagation out of the origin governed by this Hamiltonian results in the appearance of a vortex of linear polarization with the polarization perpendicular to the radial direction and a four-leaf pattern of circular polarization in $B = 0$, as well as spiral patterns of linear polarization and bell-like patterns of circular polarization in finite magnetic fields. This model qualitatively reproduces the main features of the experiment for both linear [see Figs. 2(a)–2(d)] and circular [see Figs. 2(e)–2(h)] polarizations.

This model describes the exciton polarization currents and allows us to deduce the spin currents carried by electrons and holes bound to excitons as detailed in the Supplemental Material [31]. Figures 3(b) and 3(c) show the electron and hole spin textures deduced from the measured exciton polarization texture [see Figs. 2(a) and 3(a)]. One can see that both the electron and hole spin tend to align along the effective magnetic fields given by the Dresselhaus SO interaction $\mathbf{B}_{\rm eff(}_{e)} = (2\beta_e/g_e\mu_B) \times (-k_{e,x}, k_{e,y})$, $\mathbf{B}_{\rm eff(}_{h)} = (2\beta_h/g_h\mu_B)(k_{h,x}, k_{h,y})$ [see Figs. 3(e) and 3(f)], consistent with the model. The patterns of $P_{\rm lin}$ corresponding to the simulations in Fig. 3 are shown in Fig. 2(b).

The model can be improved by including nonlinear effects. In the Supplemental Material [31], we present simulations of exciton spin currents using Gross-Pitaevskii type equations, which treat the excitons as a coherent field outside the LBS center and include dispersion and interaction. In particular, the nonlinear effects change the momenta and effective magnetic fields for

propagating excitons. The simulation results are similar to that within the density matrix approach and are in agreement with the experiment. Nonlinear spin-related phenomena form interesting perspectives for future studies. In conclusion, long-range spin currents governed by spin-orbit interaction and controlled by an applied magnetic field have been observed in a coherent exciton gas.

We thank Misha Fogler, Jorge Hirsch, Leonid Levitov, Yuriy Rubo, Lu Sham, Ben Simons, and Congjun Wu for discussions. This work was supported by DOE. The development of spectroscopy in the dilution refrigerator was also supported by ARO and NSF. A. V. K. acknowledges financial support from the Russian Ministry of Education and Science. T. O. was supported by the Ministry of Education and the Grant Agency of the Czech Republic. A. A. H. was supported by an Intel fellowship. J. R. L. was supported by a Chateaubriand Fellowship. T. C. H. L. was supported by the EU FP7 Marie Curie EPOQUES project. The collaboration was supported by EU ITN INDEX.

*jleonard@physics.ucsd.edu

[1] M. I. Dyakonov and V. I. Perel, Phys. Lett. **35A**, 459 (1971).
[2] J. E. Hirsch, Phys. Rev. Lett. **83**, 1834 (1999).
[3] S. Murakami, N. Nagaosa, and S.-C. Zhang, Science **301**, 1348 (2003).
[4] J. Sinova, D. Culcer, Q. Niu, N. A. Sinitsyn, T. Jungwirth, and A. H. MacDonald, Phys. Rev. Lett. **92**, 126603 (2004).
[5] Y. K. Kato, R. C. Myers, A. C. Gossard, and D. D. Awschalom, Science **306**, 1910 (2004).
[6] J. Wunderlich, B. Kaestner, J. Sinova, and T. Jungwirth, Phys. Rev. Lett. **94**, 047204 (2005).
[7] J. D. Koralek, C. P. Weber, J. Orenstein, B. A. Bernevig, S.-C. Zhang, S. Mack, and D. D. Awschalom, Nature (London) **458**, 610 (2009).
[8] J. M. Kikkawa and D. D. Awschalom, Nature (London) **397**, 139 (1999).
[9] C. P. Weber, N. Gedik, J. E. Moore, J. Orenstein, J. Stephens, and D. D. Awschalom, Nature (London) **437**, 1330 (2005).
[10] S. A. Crooker, M. Furis, X. Lou, C. Adelmann, D. L. Smith, C. J. Palmstrom, and P. A. Crowell, Science **309**, 2191 (2005).
[11] M. Hoesch, M. Muntwiler, V. N. Petrov, M. Hengsberger, L. Patthey, M. Shi, M. Falub, T. Greber, and J. Osterwalder, Phys. Rev. B **69**, 241401(R) (2004).
[12] M. Köning, H. Buhmann, L. W. Molenkamp, T. Hugnes, C.-X. Liu, X.-L. Qi, and S.-C. Zhang, J. Phys. Soc. Jpn. **77**, 031007 (2008).
[13] J. E. Moore, Nature (London) **464**, 194 (2010).
[14] M. Z. Hasan and C. L. Kane, Rev. Mod. Phys. **82**, 3045 (2010).
[15] A. Kavokin, G. Malpuech, and M. Glazov, Phys. Rev. Lett. **95**, 136601 (2005).
[16] C. Leyder, M. Romanelli, J. Ph. Karr, E. Giacobino, T. C. H. Liew, M. M. Glazov, A. V. Kavokin, G. Malpuech, and A. Bramati, Nat. Phys. **3**, 628 (2007).
[17] M. Maragkou, C. E. Richards, T. Ostatnický, A. J. D Grundy, J. Zajac, M. Hugues, W. Langbein, and P. G. Lagoudakis, Opt. Lett. **36**, 1095 (2011).
[18] L. E. Sadler, J. M. Higbie, S. R. Leslie, M. Vengalattore, and D. M. Stamper-Kurn, Nature (London) **443**, 312 (2006).
[19] Y.-J. Lin, K. Jiménez-García, and I. B. Spielman, Nature (London) **471**, 83 (2011).
[20] L. V. Keldysh and A. N. Kozlov, Sov. Phys. JETP **27**, 521 (1968).
[21] E. I. Rashba and E. Ya Sherman, Phys. Lett. A **129**, 175 (1988).
[22] C. Wu and I. Mondragon-Shem, arXiv:0809.3532v1.
[23] J.-W. Luo, A. N. Chantis, M. van Schilfgaarde, G. Bester, and A. Zunger, Phys. Rev. Lett. **104**, 066405 (2010).
[24] Yu. E. Lozovik and V. I. Yudson, Sov. Phys. JETP **44**, 389 (1976).
[25] T. Fukuzawa, S. S. Kano, T. K. Gustafson, and T. Ogawa, Surf. Sci. **228**, 482 (1990).
[26] M. Hagn, A. Zrenner, G. Böhm, and G. Weimann, Appl. Phys. Lett. **67**, 232 (1995).
[27] A. A. High, J. R. Leonard, A. T. Hammack, M. M. Fogler, L. V. Butov, A. V. Kavokin, K. L. Campman, and A. C. Gossard, Nature (London) **483**, 584 (2012).
[28] M. I. Dyakonov, *Spin Physics in Semiconductors* (Springer, New York, 2008).
[29] M. Z. Maialle, E. A. de Andrada e Silva, and L. J. Sham, Phys. Rev. B **47**, 15 776 (1993).
[30] J. R. Leonard, Y. Y. Kuznetsova, S. Yang, L. V. Butov, T. Ostatnický, A. Kavokin, and A. C. Gossard, Nano Lett. **9**, 4204 (2009).
[31] See the Supplemental Material at http://link.aps.org/supplemental/10.1103/PhysRevLett.110.246403 for the theory of exciton spin currents, experimental data on the temperature dependence of polarization patterns, and movies showing polarization and spin textures versus magnetic field.